

The role of decomposition reactions in assessing first-principles predictions of solid stability

Christopher J. Bartel¹, Alan W. Weimer¹, Stephan Lany², Charles B. Musgrave^{1,2,3*}, Aaron M. Holder^{1,2*}

¹Department of Chemical and Biological Engineering, University of Colorado, Boulder, Colorado 80309, USA

²National Renewable Energy Laboratory, Golden, CO 80401, USA

³Department of Chemistry and Biochemistry, University of Colorado, Boulder, Colorado 80309, USA

*Correspondence to: charles.musgrave@colorado.edu, aaron.holder@colorado.edu

ABSTRACT

The performance of density functional theory (DFT) approximations for predicting materials thermodynamics is typically assessed by comparing calculated and experimentally determined enthalpies of formation from elemental phases, ΔH_f . However, a compound competes thermodynamically with both other compounds and their constituent elemental forms, and thus, the enthalpies of the decomposition reactions to these competing phases, ΔH_d , determines thermodynamic stability. We evaluated the phase diagrams for ~56,791 compounds to classify decomposition reactions into three types: 1. those that produce elemental phases, 2. those that produce compounds, and 3. those that produce both. This analysis shows that the decomposition into elemental forms is rarely the competing reaction that determines compound stability and that approximately two-thirds of decomposition reactions involve no elemental phases. Using experimentally reported formation enthalpies for 1,012 solid compounds, we assess the accuracy of the generalized gradient approximation (GGA) (PBE) and meta-GGA (SCAN) density functionals for predicting compound stability. For 646 decomposition reactions that are not trivially the formation reaction, PBE (MAD = 70 meV/atom) and SCAN (MAD = 59 meV/atom) perform similarly, and commonly employed correction schemes using fitted elemental reference energies make only a negligible improvement (~2 meV/atom). Furthermore, for 231 reactions involving only compounds (Type 2), the agreement between SCAN, PBE, and experiment is within ~35 meV/atom and is thus comparable to the magnitude of experimental uncertainty.

INTRODUCTION

The design and discovery of new materials are being rapidly accelerated by the growing availability of density functional theory (DFT) calculated property data in open materials databases which allow users to systematically retrieve computed results for experimentally known and yet-to-be-realized solid compounds.¹⁻⁶ The primary properties of interest are the optimized structure and corresponding total energy, E , with, for example, ~50,000,000 compiled structures and energies available *via* the NOMAD repository.⁷ Given E for a set of structures, one can routinely obtain the reaction energy, E_{rxn} , to convert between structures. E for a compound is typically compared with E for its constituent elements to obtain the formation enthalpy, ΔH_f , which provides the thermodynamic driving force at zero temperature and pressure for stability of a given structure with respect to its constituent elements:

$$\Delta H_{f, A_{\alpha_1} B_{\alpha_2} \dots} = E_{A_{\alpha_1} B_{\alpha_2} \dots} - \sum_i \alpha_i E_i \quad [1]$$

where E is the calculated total energy of the compound ($A_{\alpha_1} B_{\alpha_2} \dots$), α_i the stoichiometric coefficient of element i in the compound, and E_i the total energy (chemical potential) of element i . ΔH_f computed by **Equation 1** is typically compared to ΔH_f obtained experimentally at 298 K with varying degrees of agreement depending on the density functional and compounds (chemistries) under investigation.^{2,3,8-13}

However, ΔH_f is rarely the useful quantity for evaluating the stability of a compound. More relevant are the reaction energies for a given compound relative to all other compounds within the same composition space, where the reaction with the most positive E_{rxn} is the decomposition reaction.^{11,14,15} For example, for a given ternary compound, ABC , the relevant space of competing materials includes the elements (A , B , and C), all binary compounds in the A - B , A - C , and B - C spaces, and all ternary compounds in the A - B - C space. The stability of ABC is obtained by comparing the energy of ABC with that of the linear combination of competing compounds with the same average composition – ABC – that minimizes the combined energy of the competing compounds, E_{A-B-C} . The decomposition enthalpy, ΔH_d , is then obtained by:

$$\Delta H_d = E_{rxn} = E_{ABC} - E_{A-B-C}. \quad [2]$$

$\Delta H_d > 0$ indicates an endothermic reaction for a given ABC forming from A - B - C ; the sign notation that $\Delta H_d > 0$ indicates instability is chosen to be commensurate with the commonly reported quantity, “energy above the hull”, where ΔH_d also provides the energy with respect to the convex hull but can be positive (for unstable compounds) or negative (for stable compounds). A ternary example was shown for simplicity, but the decomposition reaction and ΔH_d can be obtained for any arbitrary compound comprised of N elements by solving the N -dimensional convex hull problem.

For the high-throughput screening of new materials for a target application, stability against all competing compounds is an essential requirement for determining the viability of a candidate material.¹⁵ In

this approach, compounds are typically retained for further evaluation (more rigorous calculations or experiments) if $\Delta H_d < \gamma$, where the threshold γ commonly ranges from ~ 20 to ~ 200 meV/atom depending on the priorities of the screening approach and the breadth of materials under evaluation.¹⁶⁻²¹ The success of high-throughput screening approaches thus depends directly on the accuracy of ΔH_d , which is typically obtained using DFT with routinely employed approximations to the exchange-correlation energy. Nevertheless, despite the intimate link between stability predictions and ΔH_d , new approaches (e.g., the development of improved density functionals and/or statistical correction schemes) are primarily benchmarked against experimentally obtained ΔH_f . Here, we show that the decomposition reactions that are relevant to stability can be classified into three types, and that the ability of DFT-based approaches to predict ΔH_d for each type relative to experiment is the applicable determinant of the viability of that method for high-throughput predictions of compound stability.

RESULTS

Relevant reactions for determining the stability of compounds

The decomposition reactions that determine ΔH_d fall into one of three types: Type 1 – a given compound is the only known compound in that composition space, the decomposition products are the elements, and $\Delta H_d = \Delta H_f$ (**Fig. 1**, left); Type 2 – a given compound is bracketed (on the phase diagram) by compounds and the decomposition products are exclusively these compounds (**Fig. 1**, center); and Type 3 – a given compound is not the only known compound in the composition space, is not bracketed by compounds and the decomposition products are a combination of compounds and elements (**Fig. 1**, right). For a given compound, one of these three types of decomposition reactions will be the relevant reaction for evaluating that material's stability. Notably, these decomposition reactions apply to compounds that are stable (vertices on the convex hull, $\Delta H_d \leq 0$, **Fig. 1**, top) and unstable (above the convex hull, $\Delta H_d > 0$, **Fig. 1**, bottom).

As it pertains to thermodynamic control of synthesis, Type 2 reactions are insensitive to adjustments in elemental chemical potentials that are sometimes modulated by sputtering, partial pressure adjustments, or plasma cracking. Any changes to the elemental energies will affect the decomposition products and the compound of interest proportionally, and therefore, while ΔH_f for all compounds will change, ΔH_d will be fixed. This is in contrast to Type 1 reactions which will become more favorable with increases in the chemical potential of either element. The thermodynamics of Type 3 reactions can be modulated by these synthesis approaches if the elemental form of the species whose chemical potential is being adjusted participates in the decomposition reaction, i.e. the compound must be the nearest (within the convex hull construction) stable, or lowest energy metastable, compound to the elemental chemical potential being adjusted.²²

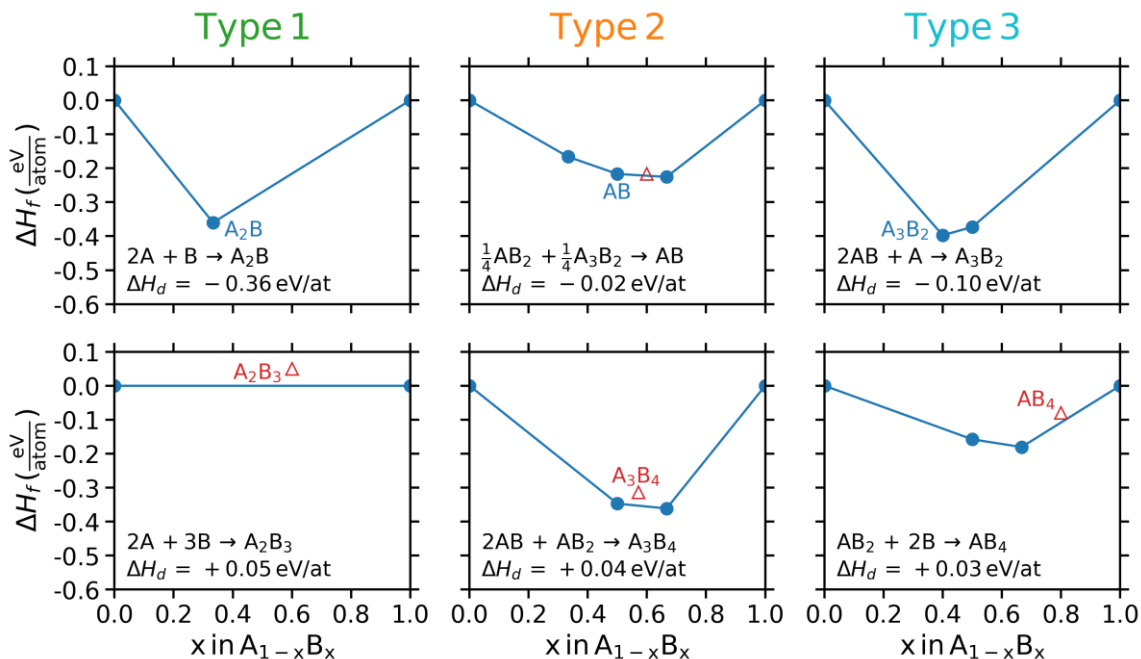


Figure 1. Three unique decomposition reactions A stable (top) and metastable (bottom) example of each reaction type. Left: reaction Type 1 – the decomposition products are the elements; Center: reaction Type 2 – the decomposition products contain no elements; Right: reaction Type 3 – the decomposition products contain elements and compounds. Solid blue circles are breaks in the hull (stable) and open red triangles are above the hull (metastable). In all examples, A and B are arbitrary elements.

The relative prevalence of each decomposition pathway is not yet known, although the phase diagrams of most inorganic crystals can be resolved using open materials databases. At present, the Materials Project¹ provides 56,791 unique inorganic crystalline solid compounds with computed ΔH_f . Using the N -dimensional convex hull construction, we determined ΔH_d and the stability-relevant decomposition reaction for each compound and report the prevalence of each reaction type in **Fig. 2**. For these 56,791 compounds, Type 2 decompositions are found to be most prevalent (63% of compounds) followed by Type 3 (34%) and Type 1 (3%). Notably, 81% of Type 1 reactions (for which $\Delta H_d = \Delta H_f$) are for binary compounds, which comprise only 13% of the Materials Project, and < 1% of the non-binary compounds compete for stability exclusively with elements (**Fig. 2**, right). As the number of unique elements in the compound, N , increases it becomes increasingly probable that other compounds will be present on the phase diagram and the decomposition will therefore be dictated by these compounds.

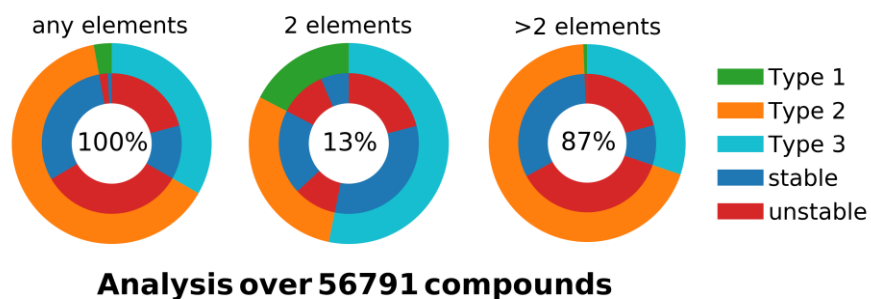


Figure 2. Prevalence of reactions among known materials Partitioning Materials Project data into each of the three decomposition reaction types (outer circle). Then, for each type, partitioning compounds as stable (on the convex hull) and unstable (above the convex hull). Left – the entire database of 56,791 compounds; Center – only binary compounds; Right – only non-binary compounds. The fraction of the Materials Project comprising each circle is shown in the interior of each diagram.

Functional performance on formation enthalpy predictions

The decomposition reactions determining compound stability that are Type 1 are the least prevalent among Materials Project compounds (~3%) suggesting that ΔH_d rarely equals ΔH_f , especially for $N > 2$. Despite this, the primary approach used to benchmark first-principles thermodynamics methods is to compare experimental and computed ΔH_f . We compared experimentally obtained ΔH_f from FactSage²³ to computed ΔH_f using the generalized gradient approximation (GGA) as formulated by Perdew, Burke, and Ernzerhof (PBE)²⁴ and using the strongly constrained and appropriately normed (SCAN)²⁵ meta-GGA density functionals for 1,012 compounds spanning 63 elements. Importantly, this reduced space of compounds with experimental thermodynamic data decompose into the full range of Type 1 (37%), 2 (22%), and 3 (41%) reactions, but first we analyze only ΔH_f for all compounds to establish a baseline for subsequent comparison to ΔH_d . On this set of 1,012 compounds, the mean absolute difference (MAD) between experimentally determined ΔH_f (at 298 K)²³ and calculated ΔH_f , nominally at 0 K and without zero-point energy (ZPE), was found to be 196 meV/atom for PBE and 88 meV/atom for SCAN (**Fig. 3a**). In addition to a reduction in the magnitude of residuals by ~55%, the distribution of residuals is nearly centered about 0 for SCAN in contrast to PBE which consistently understabilizes compounds relative to their constituent elements (particularly diatomic gases), leading to predictions of ΔH_f that are too positive by ~200 meV/atom. Unlike PBE, SCAN has been shown to perform well for a range of diversely bonded systems²⁵⁻²⁷ and does not suffer from this same systematic error.

The near zero-centered residuals produced by SCAN suggest that no global systematic difference likely exists between the energies predicted by this density functional and those obtained experimentally, and thus, some of the lingering disagreement may arise from deficiencies in the functional for describing certain types of compounds, e.g. those with transition metals,²⁷⁻³⁰ and/or be related to correlated noise in

experimental measurement. For 228 binary and ternary compounds reported in Ref. ³ (compiled from Ref. ³¹), the MAD between experimental sources (i.e., Refs. ²³ and ³¹) for ΔH_f is 30 meV/atom (**Fig. S1**). This difference agrees well with the scale of chemical accuracy expected for the experimental determination of ΔH_f of ~ 1 kcal/mol²⁷ and suggests that the disagreement between experiment and theory should not be lower than ~ 30 meV/atom on average. A potential source of disagreement between experimental and DFT-calculated ΔH_f is the incongruence in temperature, where experimental measurements are performed at 298 K and DFT calculations of ΔH_f are computed at 0 K, and thus neglect heat capacity, as well as usually neglecting ZPE. These contributions are typically assumed to be small based on the results obtained for a limited set of compounds.³² This assumption is robustly confirmed here for 647 structures where the vibrational and heat capacity effects on ΔH_f are shown to be ~ 7 meV/atom on average at 298 K (**Fig. S2**).

Optimizing elemental reference energies

Various approaches have been developed to improve the PBE prediction of ΔH_f by systematically adjusting the elemental energies, E_i , of some or all elemental phases.^{2,3,8-10} In the fitted elemental reference energy scheme, the difference between experimentally measured and calculated ΔH_f is minimized by optimally adjusting E_i by a correction term, $\delta\mu_i$:

$$\Delta H_{f, A\alpha_1 B\alpha_2 \dots} = E_{A\alpha_1 B\alpha_2 \dots} - \sum_i \alpha_i (E_i + \delta\mu_i). \quad [3]$$

To quantify the magnitude of errors that can be resolved by adjustments to the elemental reference energies, we applied **Equation 3** to ΔH_f computed with PBE and SCAN (**Fig. 3b**) with all elements considered in this optimization (these approaches are denoted in this work as PBE+ and SCAN+, respectively). Fitting reference energies for PBE approximately halves the difference between experiment and calculation and centers the residuals (MAD = 100 meV/atom). Because the difference between experiment and SCAN is less systematic, fitting reference energies improves SCAN errors less than it improves PBE, and only reduces the MAD by $\sim 20\%$ (MAD = 68 meV/atom).

While adjusting elemental reference energies is simple and effective in reducing the difference between experimentally determined and calculated ΔH_f , there are a number of limitations to this approach. Because it is a fitting scheme, the optimized $\delta\mu_i$ are sensitive to the set of experimental and calculated data used for fitting and do not necessarily have physical meaning, i.e. $\delta\mu_i$ accounts for the systematic disagreement between a density functional and experimental measurement across different types of materials, yet this can be difficult to interpret. The fitted reference energy scheme, as implemented here, produces a single $\delta\mu_i$ for each element whether a given element appears in the compounds as a cation or anion (e.g., Sb^{3+} or Sb^{3-}). For the majority of the compounds considered in this work, the use a single fitted value is appropriate because elements only appear in the data as either anions or cations. However, if one was interested in studying compounds containing elements that appear as cationic or anionic, statistically resolving a separate

$\delta\mu_i$ for cation- and anion-specific use would be more appropriate, as the fitted correction can differ in both magnitude and sign for cations and anions. Additionally, fitted reference energies have only been available for PBE (and SCAN reported in this work), so the calculation of ΔH_f using alternative functionals which may be better suited for a given problem would require a re-fitting of reference energies within that functional. These limitations make it advantageous to avoid fitted reference energies for the high-throughput prediction of stability, particularly if they have negligible effects on the validity of first-principles predictions.

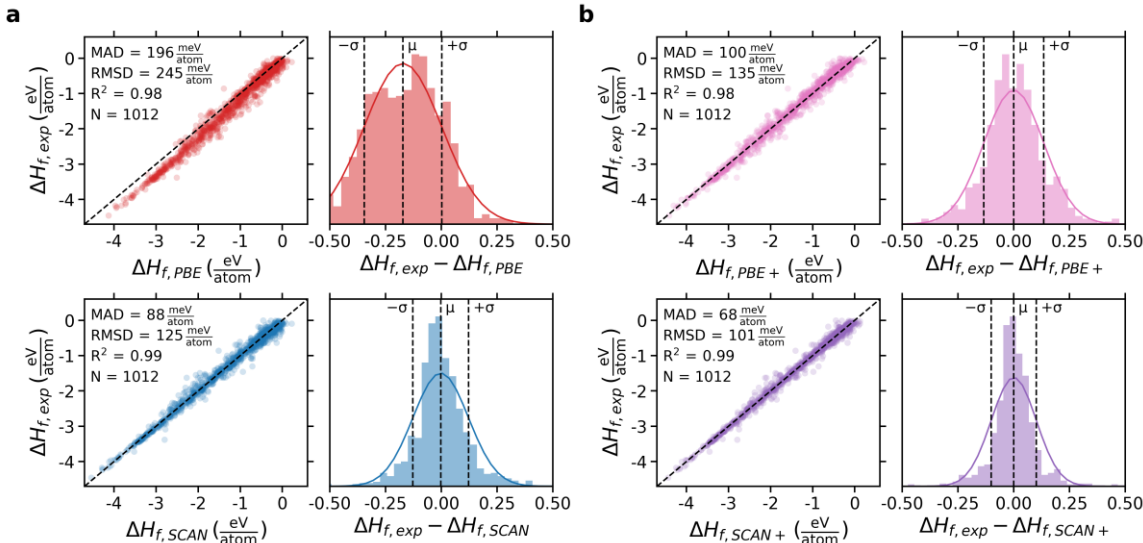


Figure 3. Experimental vs. theoretical formation enthalpies (Type 1) **a)** A comparison of experimentally measured and DFT-calculated ΔH_f for all 1,012 compounds analyzed (PBE above; SCAN below) showing that SCAN significantly improves the prediction of ΔH_f over PBE. MAD is the mean absolute difference; RMSD is the root-mean-square difference; R^2 is the correlation coefficient; N is the number of compounds shown; μ is the mean difference; σ is the standard deviation. A normal distribution constructed from μ and σ is shown as a solid curve. **b)** For the same compounds, a comparison of PBE and SCAN with experiment using fitted elemental reference energies for the calculation of ΔH_f (PBE+ above; SCAN+ below) showed that for Type 1 reactions fitted elemental reference energies significantly improve the prediction of ΔH_f , especially predictions by PBE. These results are provided in **TableS1** (for elemental energies) and **TableS2** (for compound data).

Decomposition reaction analysis

While the improved construction of the meta-GGA density functional (i.e., SCAN) and the use of fitted reference energies ameliorates errors associated with the insufficient description of the elements and thus improves the prediction of ΔH_f considerably relative to PBE, the effects these approaches have on the prediction of thermodynamic stability – i.e., ΔH_d – have not yet been quantified. We used ΔH_f obtained from experiment, PBE, and SCAN for the 1,012 compounds analyzed in **Fig. 3** to perform the N -dimensional convex hull analysis to determine the decomposition reaction and quantify ΔH_d . For 646 compounds which decompose by Type 2 or 3 reactions, the MAD between experimentally measured and DFT-computed ΔH_d is substantially lower than for ΔH_f – $\sim 60\%$ lower for PBE and $\sim 30\%$ lower for SCAN

(Fig. 4). Notably, the decomposition reaction that results from using experiment, PBE, or SCAN is identical in terms of the competing compounds and their amounts for 89% of the 1,012 compounds evaluated.

For 231 Type 2 decomposition reactions where compounds compete only with compounds and fitted reference energies thus have no influence on ΔH_d , SCAN and PBE are found to perform comparably with MADs of ~ 35 meV/atom compared with experiment on ΔH_d . This difference approaches the “chemical accuracy” of experimental measurements (~ 1 kcal/mol), the difference in ΔH_f between experimental sources (30 meV/atom), and the difference found previously for the formation of 135 ternary metal oxides from their constituent binary oxides using an approach based on PBE with a Hubbard U correction fit specifically for transition metal oxides (24 meV/atom).¹¹ Because Type 2 decomposition reactions only involve compounds, computing the decomposition reaction energy using total energies or formation enthalpies is equivalent – therefore the results with (Fig. 4a) and without (Fig. 4b) fitted reference energies are identical.

Elemental energies are included in the calculation of ΔH_d for compounds that compete thermodynamically with both compounds and elements (Type 3 decomposition reactions). However, for 415 reactions of this type and using either SCAN or PBE we found that the use of fitted reference energies does not significantly affect the agreement with experiment for ΔH_d with improvements of only ~ 2 meV/atom (Fig. 4c, d). For these compounds, SCAN improves upon PBE by $\sim 20\%$ and the MAD between SCAN and experiment (73 meV/atom) falls between those for Type 1 (88 meV/atom) and Type 2 (34 meV/atom) reactions.

The prevalence of each reaction type was quantified for the Materials Project database, with Type 2 reactions accounting for 63% of all decompositions evaluated and this fraction increasing from 29% to 67% to 75% for binary, ternary, and quaternary compounds, respectively. For these cases, our results show that both SCAN and PBE can be expected to yield chemically accurate predictions of ΔH_d , which quantifies the driving force for thermodynamic stability. While on average, SCAN and PBE perform similarly for ΔH_d , this analysis is performed only on ground-state structures within each functional. It was recently shown that SCAN performs significantly better than PBE for structure selection – i.e., identifying the correct polymorph ordering of which crystal structure is the lowest energy at fixed composition.²⁷ Here, $\sim 10\%$ of the 2,238 structures optimized were found to have different space groups using PBE and SCAN. Considering only ground-states, the lowest energy PBE and SCAN structures differ for $\sim 11\%$ of the 1,012 unique compositions assessed in this work. While the MAD from experiment for ΔH_d differs by only $\sim 20\%$ between SCAN and PBE, additional advantages when considering structure and properties are likely associated with the use of SCAN for the accurate description of compounds.^{25-27,30,33}

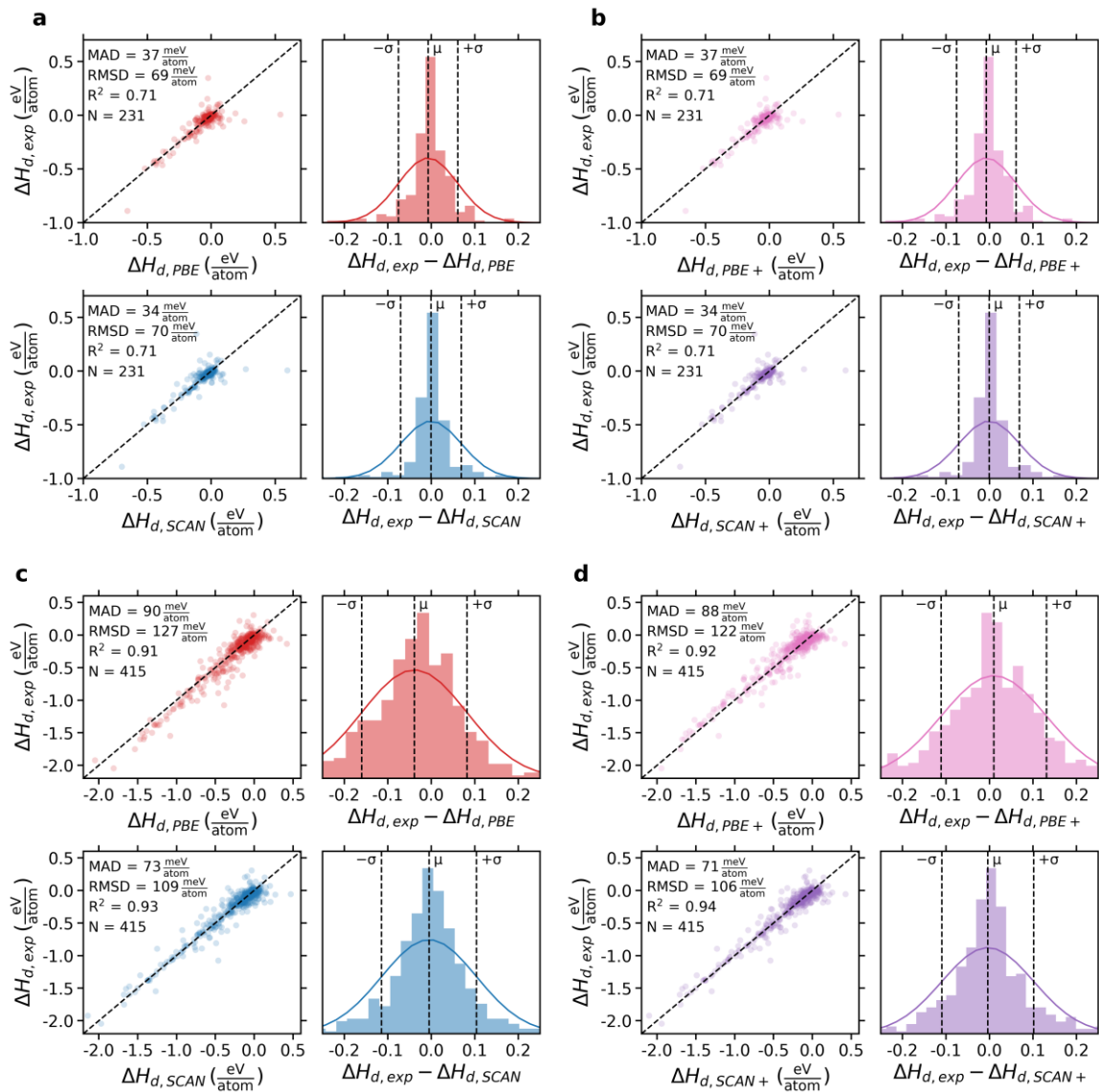


Figure 4. Experimental vs. theoretical decomposition enthalpies **a)** A comparison of experimentally measured and DFT-calculated ΔH_d (PBE above; SCAN below) for 231 compounds that undergo Type 2 decomposition reactions showing similar performance between PBE and SCAN in predicting ΔH_d . **b)** For the same compounds, a comparison of PBE and SCAN with experiment using fitted elemental reference energies for the calculation of ΔH_d (PBE+ above; SCAN+ below) showing identical results as **(a)** due to a cancellation of elemental energies for these Type 2 decomposition reactions. **c)** A comparison of experimentally measured and DFT-calculated ΔH_d (PBE above; SCAN below) for 415 compounds that undergo Type 3 decomposition showing similar performance between PBE and SCAN in predicting ΔH_d . **d)** For the same compounds, a comparison of PBE and SCAN with experiment using fitted elemental reference energies for the calculation of ΔH_d (PBE+ above; SCAN+ below) showing that adding fitted elemental reference energies does not significantly improve the prediction of ΔH_d for Type 3 decomposition reactions. Annotations are as described in the **Fig. 3** caption.

DISCUSSION

For 1,012 compounds, we show the improvement in computed formation enthalpies, ΔH_f , afforded by fitting elemental reference energies for both GGA (PBE) and meta-GGA (SCAN) density functionals (**Fig.**

3). However, to accurately predict the stability of materials it is essential to accurately compute the decomposition enthalpy, ΔH_d , which dictates stability with respect to all compounds and elements in a given chemical space. ΔH_d is computed by determining the stoichiometric decomposition reaction with the most positive reaction energy. ΔH_f is only relevant for the stability of compounds that undergo Type 1 decompositions, where the compound only competes with elemental phases and consequently, $\Delta H_d = \Delta H_f$ (**Fig. 1**). Furthermore, Type 1 decompositions occur for only 17% of binaries and almost never ($< 1\%$) for non-binaries, as shown for the $\sim 60,000$ N -component compounds evaluated (**Fig. 2**). For this reason, ΔH_f and the agreement between experiment and theory for ΔH_f are rarely relevant to the stability of materials. However, for other applications such as the calculation of defect formation energies, ΔH_f is the relevant materials property and the adjustment of calculated chemical potentials using the fitted elemental reference energy scheme may still have significant utility, especially when using PBE.

The stability of a substantial fraction of compounds, those that undergo Type 2 decompositions, can be determined without any consideration of elemental energies. For these compounds, PBE and SCAN perform similarly and approach the resolution of experimental approaches to determining ΔH_f (~ 30 meV/atom) (**Fig. 4a, Fig. S1**). Importantly, the performance metrics we provide are evaluated over a wide range of compounds and chemistries. For chemical spaces that are known to be problematic for a given approach (e.g., $3d$ transition metals for PBE), the error can significantly exceed the average difference reported here.^{27,30}

While the majority of compounds in the Materials Project compete with Type 2 decomposition reactions, this is not generally known when first evaluating a compound and so high-throughput screening approaches that typically survey a wide range of compounds will likely include analysis of Type 1 and Type 3 decomposition reactions that do require the calculation of elemental energies. Type 1 decompositions, which occur for binary compounds in sparsely explored chemical spaces, will be highly sensitive to the functional and elemental energies and SCAN improves significantly upon PBE for these compounds. Notably, fitting elemental reference energies for PBE still results in larger errors than SCAN and fitting reference energies for SCAN leads to only modest additional improvements. For Type 3 decompositions, which are $\sim 10\times$ more prevalent than Type 1 reactions in Materials Project, SCAN improves upon PBE by $\sim 20\%$ and the use of fitted elemental reference energies has almost no effect (~ 2 meV/atom on average) on either approach (**Fig. 4c, d**). Interestingly, considering the $\sim 60,000$ compounds in Materials Project (**Fig. 2**, left), a roughly equal fraction of Type 2 compounds are stable (48%) and unstable, yet only 37% of Type 3 compounds are stable. However, Type 3 compounds are more amenable to non-equilibrium synthesis approaches that allow for increased chemical potentials of the elements and potential access of metastable compounds.²²

In summary, we've shown that the decomposition reactions that dictate the stability of solid compounds can be divided into three types that depend on the presence of elemental phases in the decomposition reaction. Through a global evaluation of phase diagrams for ~60,000 compounds in the Materials Project, we quantify the prevalence of these reaction types and show that the formation enthalpy is rarely the quantity of interest for stability predictions (~3% of Materials Project compounds). Instead, the decomposition enthalpy, which may or may not include the calculation of elemental phases is the most relevant quantity. Benchmarking the PBE and SCAN density functionals against decomposition enthalpies obtained from experimental data reveals quantitatively and qualitatively different results than benchmarking only against formation enthalpies and in most cases mitigates the need to systematically correct DFT-calculated elemental energies for the assessment of stability. We showed that for 231 reaction energies between compounds, the agreement between SCAN, PBE, and experiment (~35 meV/atom) is comparable to the expected noise in experimental measurements. Therefore, because this type of decomposition reaction is predominant in determining solid stability, we show that high-throughput DFT approaches to stability predictions are generally in excellent agreement with experiment. For alternative decomposition reactions that include both compounds and elements or problems that require higher energy resolution such as polymorph energy ordering,^{28,34} the choice of functional (e.g., SCAN instead of PBE) can have non-negligible effects on stability predictions.

METHODS

Experimental values for ΔH_f were obtained from the FactSage database²³ for 1,012 compounds as reported at 298 K and 1 atm. For each compound, the NREL Materials Database (NRELMatDB)³⁵ was queried for structures matching the composition within 50 meV/atom of the ground-state structure as reported in the database. If a given compound had no calculated structures tabulated in NRELMatDB, the procedure was repeated with the Materials Project database¹. Structures containing potentially magnetic elements were sampled in non-magnetic, two ferromagnetic (high- and low-spin), and up to 16 antiferromagnetic configurations (depending on cell configuration) where the ground-state magnetic configuration was retained for each structure. Sampling was performed using the approach described by NRELMatDB. This process was also repeated for all 63 elements represented in the dataset with the exception of H₂, N₂, O₂, F₂, and Cl₂ which were calculated as diatomic molecules in a 15 × 15 × 15 Å box. After magnetic sampling, 2,238 unique structures were found for the 1,012 compounds and 63 elements. All structures were optimized with PBE and SCAN using the Vienna Ab Initio Simulation Package (VASP)^{36,37} using the projector augmented wave (PAW) method^{38,39}, a plane wave energy cutoff of 520 eV, and a Γ -centered Monkhorst-Pack k-point grid with $N = 20|b_i|$ discretizations along each reciprocal lattice vector, b_i . The energy cutoff, k-point density, and related convergence settings were sufficient to achieve

total energy convergence of < 5 meV/atom for all calculations. Pseudopotentials used for each element are provided in **TableS1**. For the calculation of phonons to compute thermal effects, the finite displacement method with $2 \times 2 \times 2$ supercells as implemented in PHONOPY⁴⁰ was used with SCAN and an increased plane wave cutoff of 600 eV and further tightened convergence criteria for total energy convergence of < 1 meV/atom. These results are compiled in **TableS3**.

SUPPLEMENTARY INFORMATION

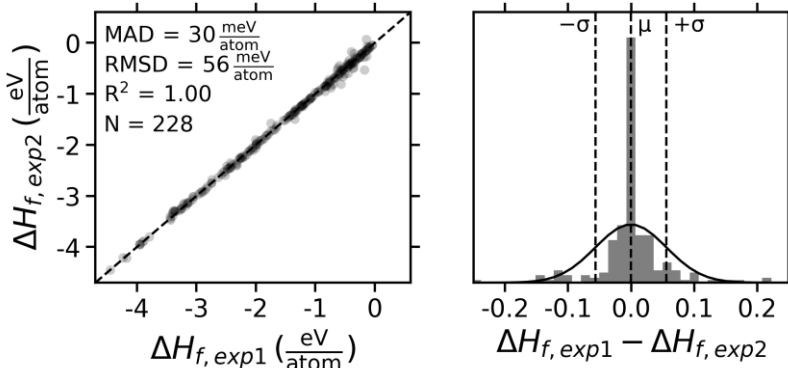


Figure S1. Uncertainty in experimentally obtained formation enthalpies Comparing formation enthalpies from two experimental sources – exp1 = Ref. ²³; exp2 = Ref. ³¹.

Phonon effects on formation enthalpy

A key difference between experimental and DFT-calculated ΔH_f is the incongruence in temperature, where experimental measurements are performed at 298 K and DFT calculations of ΔH_f are computed at 0 K, that is neglecting heat capacity, and without zero-point energy (ZPE) (**Equation 1**). To approximate $\Delta H_f(298 \text{ K})$ within DFT, we applied the following equations to 647 SCAN-calculated structures:

$$\Delta H_{f,298}(A_{\alpha_1}B_{\alpha_2} \dots) = E_{298}(A_{\alpha_1}B_{\alpha_2} \dots) - \sum_i \alpha_i E_{i,298} \quad [\text{S1}]$$

$$E_{298}(A_{\alpha_1}B_{\alpha_2} \dots) = E + E_{ZPE} + \int_0^{298} C_V(T) dT \quad [\text{S2}]$$

$$E_{i,298} = E_i + E_{ZPE} + \int_0^{298} C_{V_i}(T) dT \quad [\text{S3}]$$

where E_{ZPE} is the ZPE and C_V is the constant-volume specific heat. These contributions are typically assumed to be negligible and justified from the results obtained for a limited set of compounds.³² This assumption is confirmed here for these 647 structures (**Fig. S2a**). Importantly, E_{ZPE} and the temperature-dependence of C_V often have non-negligible magnitude (~ 50 meV/atom each on average – **Fig. S2b,c**), yet there is near-perfect cancellation between these contributions to the enthalpy for the compounds and for the elements such that the MAD between calculated $\Delta H_f(298 \text{ K})$ and $\Delta H_f(0 \text{ K}) - E_{ZPE}$ is only 7 meV/atom using SCAN. Importantly, we recently showed that for the Gibbs formation energy, $\Delta G_f(T)$, the effects of

temperature do not cancel well between elements and compounds of different phase (solid, liquid, or gas) as a result of an incomplete cancellation of vibrational entropy, even when the chemical potential(s) of the non-solid elements are accounted for using experimental data.⁴¹

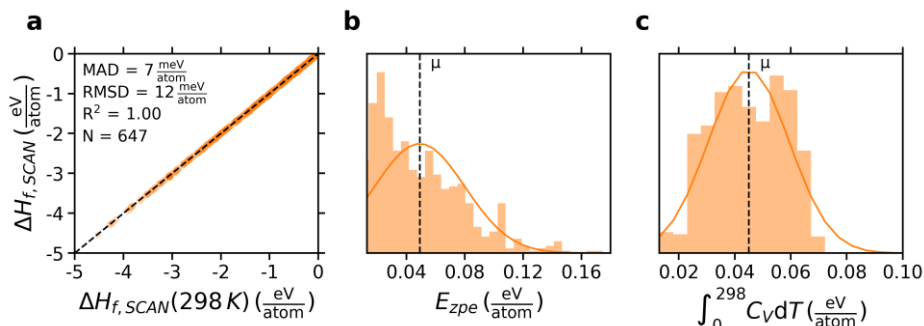


Figure S2. Phonon effects on formation enthalpy **a)** A comparison of ΔH_f computed using SCAN with ($\Delta H_{f,SCAN}(298\text{ K})$) and without ($\Delta H_{f,SCAN}$) phonon effects on the enthalpy at 298 K demonstrating that zero-point energy and heat capacity have negligible effect on the formation enthalpy of compounds. Annotations are as described in the **Fig. 3** caption. **b)** Distribution of zero-point energies for the 647 structures shown in **(a)**. **c)** Distribution of the thermal effects of heat capacity at 298 K on the enthalpy of formation for the 647 structures shown in **(a)**. These results are provided in **TableS3**.

TableS1. See *mus.csv*. el = elements; pp = pseudopotential; PBE = energy calculated with PBE; PBE+ = fitted reference energy for PBE; SCAN = energy calculated with SCAN; SCAN+ = fitted reference energy for SCAN. All units are eV/atom.

TableS2. See *Hs.csv*. formula = chemical formula; _PBE = calculated with PBE; _SCAN = calculated with SCAN; _PBE+ = calculated with PBE and fitted reference energies; _SCAN+ = calculated with SCAN and fitted reference energies; E = total energy; sg = spacegroup; dHf = formation enthalpy; dHd = decomposition enthalpy; type = decomposition reaction type. All units are eV/atom.

TableS3. See *phonons.csv*. formula = chemical formula; sg = spacegroup; E = total energy per atom; zpe = zero-point energy; CvdT = integrated specific heat from 0 K to 298 K; dH0 = formation enthalpy without phonon effects; dH298 = formation enthalpy with thermal effects (zpe and CvdT). All units are eV/atom.

Data availability

All necessary data for reproducing this work is contained within, including the computed formation enthalpies, decomposition enthalpies, and chemical potentials that are provided in the Supplementary Information. Additional data are available from the corresponding author upon request.

Acknowledgements

The authors gratefully acknowledge Vladan Stevanović for many useful discussions on the thermodynamics of solids and thank Christopher Sutton and Jacob Clary for providing feedback on the manuscript. This work was supported by the National Science Foundation (award no. CHE-1800592 and CBET-1806079). The authors also acknowledge partial support for this work from the U.S. Department of Energy, Office of Basic Energy Sciences (S.L. and A.M.H., contract no. DE-AC36-08GO28308) and Fuel Cell Technologies Office (A.W.W. and C.B.M, award no. DE-EE0008088). High Performance Computing resources were sponsored by the U.S. Department of Energy's Office of Energy Efficiency and Renewable Energy, located at NREL.

Contributions

C.J.B. performed the calculations and analysis and drafted the manuscript. A.W.W provided the experimental dataset and assisted in its curation. S.L., C.B.M. and A.M.H supervised the project, provided guidance on the calculations and analysis, and assisted in writing the manuscript. All authors commented on the results and reviewed the manuscript.

Competing interests

The authors declare no competing interests.

Corresponding authors

Correspondence to Charles Musgrave (charles.musgrave@colorado.edu) or Aaron Holder (aaron.holder@colorado.edu)

REFERENCES

- 1 Jain, A. *et al.* Commentary: The Materials Project: A materials genome approach to accelerating materials innovation. *APL Materials* **1**, 011002, doi:10.1063/1.4812323 (2013).
- 2 Kirklin, S. *et al.* The Open Quantum Materials Database (OQMD): assessing the accuracy of DFT formation energies. *npj Computational Materials* **1**, 15010 (2015).
- 3 Stevanović, V., Lany, S., Zhang, X. & Zunger, A. Correcting density functional theory for accurate predictions of compound enthalpies of formation: Fitted elemental-phase reference energies. *Physical Review B* **85**, 115104 (2012).
- 4 Curtarolo, S. *et al.* AFLOWLIB.ORG: A distributed materials properties repository from high-throughput ab initio calculations. *Computational Materials Science* **58**, 227-235, doi:<https://doi.org/10.1016/j.commatsci.2012.02.002> (2012).
- 5 Pizzi, G., Cepellotti, A., Sabatini, R., Marzari, N. & Kozinsky, B. AiiDA: automated interactive infrastructure and database for computational science. *Computational Materials Science* **111**, 218-230, doi:<https://doi.org/10.1016/j.commatsci.2015.09.013> (2016).
- 6 Sun, W. *et al.* A Map of the Inorganic Ternary Metal Nitrides. *Preprint at* <https://arxiv.org/abs/1809.09202> (2018).
- 7 Draxl, C. & Scheffler, M. NOMAD: The FAIR Concept for Big-Data-Driven Materials Science. *Preprint at* <https://arxiv.org/abs/1805.05039> (2018).
- 8 Lany, S. Semiconductor thermochemistry in density functional calculations. *Physical Review B* **78**, 245207 (2008).
- 9 Wang, L., Maxisch, T. & Ceder, G. Oxidation energies of transition metal oxides within the $\text{GGA}+\text{U}$ framework. *Physical Review B* **73**, 195107, doi:10.1103/PhysRevB.73.195107 (2006).
- 10 Jain, A. *et al.* Formation enthalpies by mixing GGA and GGA+ U calculations. *Physical Review B* **84**, 045115 (2011).
- 11 Hautier, G., Ong, S. P., Jain, A., Moore, C. J. & Ceder, G. Accuracy of density functional theory in predicting formation energies of ternary oxides from binary oxides and its implication on phase stability. *Physical Review B* **85**, 155208, doi:10.1103/PhysRevB.85.155208 (2012).
- 12 Sun, W. *et al.* The thermodynamic scale of inorganic crystalline metastability. *Science Advances* **2**, doi:10.1126/sciadv.1600225 (2016).
- 13 Pandey, M. & Jacobsen, K. W. Heats of formation of solids with error estimation: The mBEEF functional with and without fitted reference energies. *Physical Review B* **91**, 235201, doi:10.1103/PhysRevB.91.235201 (2015).
- 14 Ong, S. P., Wang, L., Kang, B. & Ceder, G. Li-Fe-P-O₂ Phase Diagram from First Principles Calculations. *Chemistry of Materials* **20**, 1798-1807, doi:10.1021/cm702327g (2008).
- 15 Zunger, A. Inverse design in search of materials with target functionalities. *Nature Reviews Chemistry* **2**, 0121, doi:10.1038/s41570-018-0121 (2018).
- 16 Ryan, J., Tam, M., John, B. & Dane, M. Material Discovery and Design Principles for Stable, High Activity Perovskite Cathodes for Solid Oxide Fuel Cells. *Advanced Energy Materials* **8**, 1702708, doi:10.1002/aenm.201702708 (2018).

- 17 Korbek, S., Marques, M. A. L. & Botti, S. Stable hybrid organic-inorganic halide perovskites for photovoltaics from ab initio high-throughput calculations. *Journal of Materials Chemistry A* **6**, 6463-6475, doi:10.1039/C7TA08992A (2018).
- 18 Isaacs, E. B. & Wolverton, C. Inverse Band Structure Design via Materials Database Screening: Application to Square Planar Thermoelectrics. *Chemistry of Materials* **30**, 1540-1546, doi:10.1021/acs.chemmater.7b04496 (2018).
- 19 Lu, Z. & Ciucci, F. Anti-perovskite cathodes for lithium batteries. *Journal of Materials Chemistry A* **6**, 5185-5192, doi:10.1039/C7TA11074J (2018).
- 20 Dagdelen, J., Montoya, J., de Jong, M. & Persson, K. Computational prediction of new auxetic materials. *Nature Communications* **8**, 323, doi:10.1038/s41467-017-00399-6 (2017).
- 21 Singh, A. K., Mathew, K., Zhuang, H. L. & Hennig, R. G. Computational Screening of 2D Materials for Photocatalysis. *The journal of physical chemistry letters* **6**, 1087-1098, doi:10.1021/jz502646d (2015).
- 22 Sun, W. *et al.* Thermodynamic Routes to Novel Metastable Nitrogen-Rich Nitrides. *Chemistry of Materials* **29**, 6936-6946, doi:10.1021/acs.chemmater.7b02399 (2017).
- 23 Bale, C. W. *et al.* FactSage thermochemical software and databases, 2010–2016. *Calphad* **54**, 35-53, doi:<http://dx.doi.org/10.1016/j.calphad.2016.05.002> (2016).
- 24 Perdew, J. P., Burke, K. & Ernzerhof, M. Generalized Gradient Approximation Made Simple. *Physical Review Letters* **77**, 3865-3868, doi:10.1103/PhysRevLett.77.3865 (1996).
- 25 Sun, J., Ruzsinszky, A. & Perdew, J. P. Strongly Constrained and Appropriately Normed Semilocal Density Functional. *Physical Review Letters* **115**, 036402, doi:10.1103/PhysRevLett.115.036402 (2015).
- 26 Sun, J. *et al.* Accurate first-principles structures and energies of diversely bonded systems from an efficient density functional. *Nature Chemistry* **8**, 831, doi:10.1038/nchem.2535 (2016).
- 27 Zhang, Y. *et al.* Efficient first-principles prediction of solid stability: Towards chemical accuracy. *npj Computational Materials* **4**, 9, doi:10.1038/s41524-018-0065-z (2018).
- 28 Sai Gautam, G. & Carter, E. A. Evaluating transition metal oxides within DFT-SCAN and SCAN+U frameworks for solar thermochemical applications. *Physical Review Materials* **2**, 095401, doi:10.1103/PhysRevMaterials.2.095401 (2018).
- 29 Ekholm, M. *et al.* Assessing the SCAN functional for itinerant electron ferromagnets. *Physical Review B* **98**, 094413, doi:10.1103/PhysRevB.98.094413 (2018).
- 30 Isaacs, E. B. & Wolverton, C. Performance of the strongly constrained and appropriately normed density functional for solid-state materials. *Physical Review Materials* **2**, 063801, doi:10.1103/PhysRevMaterials.2.063801 (2018).
- 31 Kubaschewski, O., Alcock, C. B. & Spencer, P. J. *Materials thermochemistry*. 6th edn, (Pergamon Press, 1993).
- 32 Bachmann, K. J., Hsu, F. S. L., Thiel, F. A. & Kasper, H. M. Debye temperature and standard entropies and enthalpies of compound semiconductors of the type I-III-VI₂. *Journal of Electronic Materials* **6**, 431-448, doi:10.1007/bf02660497 (1977).
- 33 Kitchaev, D. A. *et al.* Energetics of MnO_2 polymorphs in density functional theory. *Physical Review B* **93**, 045132, doi:10.1103/PhysRevB.93.045132 (2016).
- 34 Kitchaev, D. A. *et al.* Energetics of MnO_2 polymorphs in density functional theory. *Physical Review B* **93**, 045132, doi:10.1103/PhysRevB.93.045132 (2016).
- 35 Filip, M. R. & Giustino, F. The geometric blueprint of perovskites. *Proceedings of the National Academy of Sciences* **115**, 5397-5402, doi:10.1073/pnas.1719179115 (2018).
- 36 Kresse, G. & Furthmüller, J. Efficient iterative schemes for ab initio total-energy calculations using a plane-wave basis set. *Physical Review B* **54**, 11169-11186, doi:10.1103/PhysRevB.54.11169 (1996).
- 37 Kresse, G. & Furthmüller, J. Efficiency of ab-initio total energy calculations for metals and semiconductors using a plane-wave basis set. *Computational Materials Science* **6**, 15-50, doi:[https://doi.org/10.1016/0927-0256\(96\)00008-0](https://doi.org/10.1016/0927-0256(96)00008-0) (1996).
- 38 Kresse, G. & Joubert, D. From ultrasoft pseudopotentials to the projector augmented-wave method. *Physical Review B* **59**, 1758-1775, doi:10.1103/PhysRevB.59.1758 (1999).
- 39 Blöchl, P. E. Projector augmented-wave method. *Physical Review B* **50**, 17953-17979, doi:10.1103/PhysRevB.50.17953 (1994).
- 40 Togo, A. & Tanaka, I. First principles phonon calculations in materials science. *Scripta Materialia* **108**, 1-5, doi:<https://doi.org/10.1016/j.scriptamat.2015.07.021> (2015).
- 41 Bartel, C. J. *et al.* Physical descriptor for the Gibbs energy of inorganic crystalline solids and temperature-dependent materials chemistry. *Nature Communications* **9**, 4168, doi:10.1038/s41467-018-06682-4 (2018).

